Am J Physiol Lung Cell Mol Physiol 318: L180–L191, 2020.
First published November 6, 2019; doi:10.1152/ajplung.00039.2019.

RESEARCH ARTICLE

Amphiregulin modulates murine lung recovery and fibroblast function following exposure to agriculture organic dust

Jill A. Poole,[1] Tara M. Nordgren,[2] Art J. Heires,[1] Amy J. Nelson,[1] Dawn Katafiasz,[1] Kristina L. Bailey,[1,3] and Debra J. Romberger[1,3]

[1]*Pulmonary, Critical Care, Sleep & Allergy Division, Department of Internal Medicine, University of Nebraska Medical Center, Omaha, Nebraska;* [2]*Division of Biomedical Sciences, School of Medicine, University of California, Riverside, California; and* [3]*Veterans Affairs Nebraska-Western Iowa Health Care System, Omaha, Nebraska*

Submitted 23 January 2019; accepted in final form 29 October 2019

Poole JA, Nordgren TM, Heires AJ, Nelson AJ, Katafiasz D, Bailey KL, Romberger DJ. Amphiregulin modulates murine lung recovery and fibroblast function following exposure to agriculture organic dust. *Am J Physiol Lung Cell Mol Physiol* 318: L180–L191, 2020. First published November 6, 2019; doi:10.1152/ajplung.00039.2019.—Exposure to agricultural bioaerosols can lead to chronic inflammatory lung diseases. Amphiregulin (AREG) can promote the lung repair process but can also lead to fibrotic remodeling. The objective of this study was to determine the role of AREG in altering recovery from environmental dust exposure in a murine in vivo model and in vitro using cultured human and murine lung fibroblasts. C57BL/6 mice were intranasally exposed to swine confinement facility dust extract (DE) or saline daily for 1 wk or allowed to recover for 3–7 days while being treated with an AREG-neutralizing antibody or recombinant AREG. Treatment with the anti-AREG antibody prevented resolution of DE exposure-induced airway influx of total cells, neutrophils, and macrophages and increased levels of TNF-α, IL-6, and CXCL1. Neutrophils and activated macrophages ($CD11c^{+}$ $CD11b^{hi}$) persisted after recovery in lung tissues of anti-AREG-treated mice. In murine and human lung fibroblasts, DE induced the release of AREG and inflammatory cytokines. Fibroblast recellularization of primary human lung mesenchymal matrix scaffolds and wound closure was inhibited by DE and enhanced with recombinant AREG alone. AREG treatment rescued the DE-induced inhibitory fibroblast effects. AREG intranasal treatment for 3 days during recovery phase reduced repetitive DE-induced airway inflammatory cell influx and cytokine release. Collectively, these studies demonstrate that inhibition of AREG reduced, whereas AREG supplementation promoted, the airway inflammatory recovery response following environmental bioaerosol exposure, and AREG enhanced fibroblast function, suggesting that AREG could be targeted in agricultural workers repetitively exposed to organic dust environments to potentially prevent and/or reduce disease.

agriculture; amphiregulin; dust; fibroblast; inflammation; lung; recovery; repair

INTRODUCTION

Chronic inhalation of organic dust causes significant airway inflammatory diseases, including nonallergic asthma, chronic bronchitis, and chronic obstructive pulmonary disease, particularly in agriculture workers (10, 51). Organic dusts/dust extracts from animal confinement facilities are complex and contain an abundant and wide diversity of gram-positive and gram-negative bacterial components (3, 21, 22), proteases (40), and particulates that have been shown to elicit airway neutrophil influx and proinflammatory mediator release through engagement of Toll-like receptor (TLR)/MyD88 signaling pathways in mice (7, 32, 33, 34). Genetic polymorphisms in TLRs have also been demonstrated to modify human airway disease manifestations in exposed persons (11, 43, 44). However, therapeutic strategies targeting these signaling pathways in humans remain elusive, and currently, no treatments exist to significantly reverse exposure-induced lung disease and progressive respiratory impairment. The epidermal growth factor receptor signaling pathway is required for the proinflammatory responses of bronchial epithelial cells (5, 9), and we recently reported that the epidermal growth factor receptor agonist amphiregulin (AREG) has a role in repair and recovery processes in the lung because AREG enhanced bronchial epithelial cell repair capacities and rescued dust extract-induced epithelial recellularization deficits (23). Moreover, lung levels of AREG have also been found to be upregulated during normative recovery following repetitive dust exposure in mice (48).

Dysregulation of lung repair processes is a key feature of numerous lung diseases (4, 45, 50), and AREG has been characterized as both protective and injurious in the progression of various lung diseases (2, 13, 18, 24, 37, 46). AREG can promote proresolution effector cell function and epithelial repair process, but overexpression can lead to fibrotic remodeling (2). AREG expression has been shown to be enhanced by classically activated M1 macrophages through TLR4/MAPK signaling pathways (55). AREG displays bifunctional properties in that it promotes the growth of fibroblasts and tumor cells (25), but it can also inhibit the growth of some normal and neoplastic cell lines (26). In chronic obstructive pulmonary disease and tobacco smoke exposure, fibroblast activity and proliferation is generally reduced (16, 35, 36), and in contrast, fibroblasts are generally hyperproliferative in diseases, such as idiopathic pulmonary fibrosis (14, 49, 53). With regard to other environmental exposures, fibroblast function is decreased with ultrafine carbon black particle (17) and cerium oxide nanoparticle (19) exposures, whereas silicosis and endotoxin appear to increase fibroblast migration and proliferation (6, 12). Early studies found increased basement membrane thickening in exposed agriculture workers (42), and animal studies demonstrate increased collagen deposition and fibronectin release (31), which suggest a potential role for fibroblast processes.

Address for reprint requests and other correspondence: J. A. Poole, 985990 Nebraska Medical Center, Omaha, NE 68198-5990.

Therefore, the first objective of this study was to investigate whether reducing endogenous AREG would impact recovery responses in vivo in the setting of repeated agricultural organic dust extract (DE) exposure. The second objective of this study was to investigate the effect of agriculture-derived DE exposure on lung fibroblast functions and determine whether AREG modulates these responses. We hypothesized that blocking AREG would impair the normative repair response to DE exposure and that recombinant AREG treatment would reverse DE-induced fibroblast dysfunction. To test these hypotheses, we utilized a mouse model of DE-induced lung inflammation and recovery employing an AREG-neutralizing antibody to determine its impact on inflammatory and resolution mediators. Next, we used a decellularized lung scaffolding model and primary human lung fibroblasts to test fibroblast responses to DE and AREG. Together, these investigations identify a role for AREG in regulating lung recovery processes following organic dust exposure and establish a role for lung fibroblasts.

METHODS

Dust extract. Environmental dust was collected and prepared as previously described (30, 31). Briefly, settled dust was collected from horizontal surfaces greater than 1 m above the floor in concentrated swine feeding operations housing 500–800 animals. Dust was sifted through a coarse strainer and extracted in Hanks' balanced salt solution (100 mg/mL). The saturated solution was incubated at room temperature for 1 h with stirring, centrifuged twice for 20 min at 2,000 × *g*, and the final supernatant was filter sterilized (0.22 μm), a process that also removes coarse particles. Stock (100%) DE aliquots were frozen at −20°C until use in experiments and diluted in sterile phosphate-buffered saline (PBS; pH: 7.4) to a final concentration of 12.5% (vol/vol) for animal studies and 5% for fibroblast studies. The 12.5% DE concentration in 50 μL volume has been previously shown to elicit optimal lung inflammation in mice and is well tolerated (33). These diluted extracts contained ~4 mg/mL of total protein as measured by nanodrop spectrophotometry (NanoDrop Technologies, Wilmington, DE). The endotoxin concentration of 12.5% DE ranged from 155 to 175 EU/mL and 5% DE ranged from 62 to 70 EU/mL as determined by the limulus amebocyte lysate assay (Millipore-Sigma). Dust extracts from at least three different sources were used in these experiments.

Animal model. Male and female C57BL/6 mice (at least 8 wk old) were purchased from The Jackson Laboratory (Bar Harbor, ME). All animal procedures were approved by the Institutional Animal Care and Use Committee at the University of Nebraska Medical Center and were in accordance with the NIH guidelines for the use of rodents. Per established protocol, mice were lightly anesthetized by isoflurane inhalation before intranasal instillation of 50 μL sterile saline (PBS) or 12.5% DE (33). This model has also been utilized by other investigators to model agriculture environmental exposure-induced airway disease in mice (20, 38, 39). Mice were challenged with six doses of DE (or saline) over an 8-day period and euthanized at 5 h following the final DE challenge ("exposure phase") or allowed to recover for 7 days without DE ("recovery phase"). During the exposure and recovery phases, mice were injected intraperitoneally five times with 100 μg of an AREG-neutralizing antibody (antimurine AREG, BSA and azide free, ab31344, Abcam, Cambridge, MA) in 250 μL saline, or 100 μg of an isotype control antibody (ab171870, Abcam) in 250 μL, before and during the recovery phase (every third day, "recovery" groups; see Fig. 1*A*). In separate studies, mice challenged with 8 doses of DE over a 10-day period were then treated with 1 μg of intranasal recombinant murine AREG (R&D Systems, 989-AR) in 50 μL saline or vehicle control daily for 3 days (without DE) to determine whether direct AREG delivery would hasten resolution of inflammation (Fig. 1*B*). No differences in body weight gain were observed between treatment groups during these experiments.

Bronchoalveolar lavage. Following euthanasia, mouse lungs were lavaged with three 1-mL aliquots of sterile PBS. Bronchoalveolar lavage fluid (BALF) was collected, and total cell counts from pooled lavages were enumerated by hemocytometer. Differential cell counts

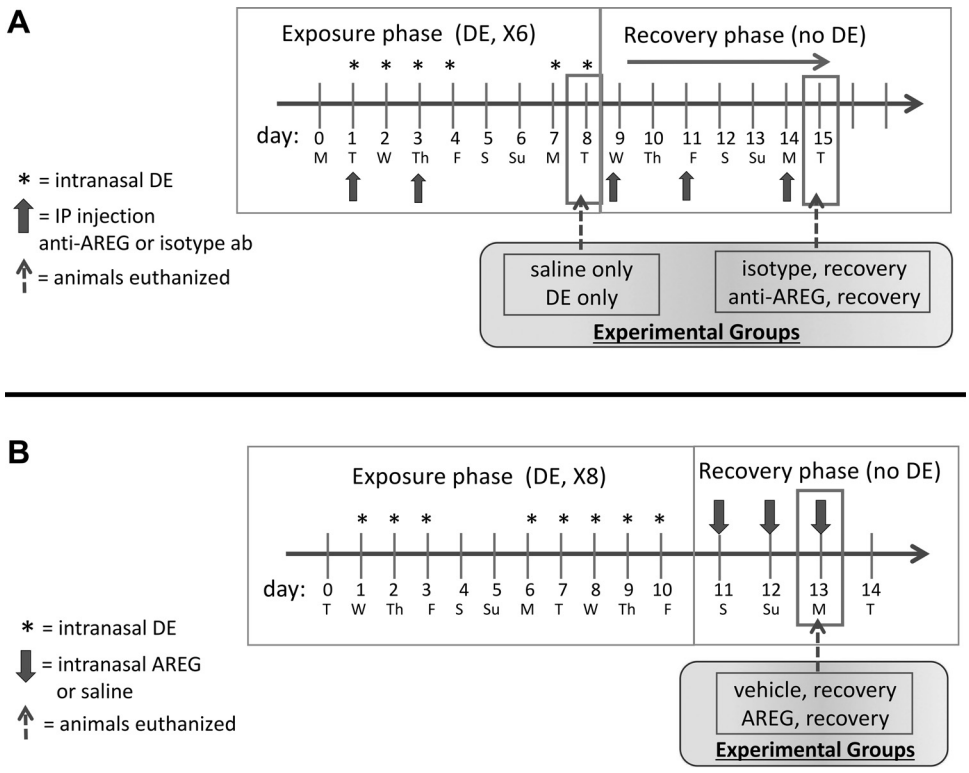

Fig. 1. Experimental design. Mice (8 per group, 4 male, 4 female) were exposed to intranasal (i.n.) dust extract (DE) or saline vehicle on 6 consecutive weekdays and were then euthanized 5 h after the final exposure (*A*, exposure phase). Mice challenged with DE as above were allowed to recover for an additional 7 days (*A*, recovery) while being treated with an anti-amphiregulin (AREG) or isotype control antibody (5 treatments ip) during both exposure and recovery phases. Mice were euthanized on *day 7* of recovery. In separate experiments, mice (6 per group, male) were challenged with i.n. DE for 8 days, then allowed to recover for 3 days with daily i.n. recombinant AREG treatment, and were euthanized 5 h after the final AREG dose (*B*).

were quantified microscopically on cytocentrifuge slides (Cytopro, ELITechGroup, Logan, UT) stained with DiffQuick (Siemens, Newark, DE).

Cytokine/chemokine assay. Cell-free BALF from the first lavage fraction was evaluated for cytokines and chemokines by murine-specific enzyme-linked immunosorbent assays (ELISA). Levels of mediators involved in DE-induced airway inflammation, including TNF-α, IL-6, and the murine neutrophil chemoattractant CXCL1 (52), in addition to the lung repair-associated mediators, AREG and IL-10, were quantitated by commercially available kits (Duoset ELISA development kits, R&D Systems, Minneapolis, MN) according to manufacturer's instructions. Limits of detectability for each mediator were 25, 35, 15, 20, and 12 pg/mL for TNF, IL-6, CXCL1, AREG, and IL-10, respectively.

Serum IL-10 and AREG. Whole blood was collected following euthanasia from the axillary artery and placed in BD Microtainer Tubes (Becton Dickinson, Franklin Lakes, NJ) and centrifuged, and cell-free serum was collected. Serum IL-10 and AREG levels were quantified by ELISA kits as above, according to the manufacturer's instructions.

Histopathology. Following lung lavage, right lungs were excised and inflated to 15 cm H_2O pressure with 10% formalin (Sigma) to preserve pulmonary architecture. Lungs were embedded in paraffin, and sections (4–5 μm) were cut and stained with hematoxylin and eosin and microscopically reviewed in a blinded manner.

Cell staining and flow cytometry. Left lung tissues were harvested after the right ventricle was infused with 10 mL of sterile PBS with heparin (1.5 U/mL; Sigma) to remove blood from the pulmonary vasculature. Lung tissues were subjected to an automated dissociation procedure using the gentleMACS tissue dissociator (Miltenyi Biotech, Auburn, CA) and digested as previously described (30, 31). After passing the cell suspension through a 40 μm nylon mesh (Fisher), red blood cells were lysed in ACK Lysing Buffer (Quality Biological Inc, Gaithersburg, MD) for 2 min at room temperature, and cells were resuspended in DMEM. Viability of the lung cells was assessed by trypan blue exclusion and LIVE/DEAD Fixable Blue Dead Cell Stain Kit (Invitrogen by Thermo Fisher Scientific). Ultimately, less than 1% of gated cells were not viable, with no difference in viability noted between treatment conditions (data not shown). Total cells in lung homogenates for each animal were enumerated using a TC20 automated cell counter (Bio-Rad, Hercules, CA).

Lung cells from each animal were incubated with CD16/32 (Fc Block, BD Biosciences) to minimize nonspecific antibody staining and then stained with monoclonal antibodies directed against rat anti-mouse CD45 (clone 30-F11), CD11b (clone M1/70), Ly6G (clone 1A8), CD4 (clone RM 4–5), CD8a (clone 53–6.7), and hamster anti-mouse CD3 (clone 145–2C11), rat anti-mouse CD19 (clone eBio1D3), and CD11c (clone N418). Antibodies were obtained for CD45 and CD19 from eBiosciences, CD11b and Ly6G from BD Biosciences, CD11c from Invitrogen, and the remainder from BD Biosciences. Gating strategies for $CD11c^+CD11b^{lo}$ alveolar macrophages, $CD11c^+CD11b^{hi}$ exudative macrophages, $Ly6G^+$ neutrophils, $CD3^+CD4^+$ and $CD3^+CD8^+$ T cells, and $CD3^-CD19^+$ B cells were previously reported (28–30). The percentage of all respective cell populations was determined from live $CD45^+$ lung leukocytes after excluding debris and doublets. This percentage was multiplied by the respective total lung cell numbers to determine specific cell population numbers for each animal.

Primary lung fibroblast culture. Primary murine lung fibroblasts (MLF) were isolated from mouse lung tissues as previously described (16) and cultured in DMEM, supplemented with 10% FCS, 50 U/mL penicillin G sodium, and 50 μg/mL streptomycin sulfate for 3 wk. Primary human lung fibroblasts (HLF) were isolated from deidentified normal lungs obtained from the International Institute for the Advancement of Medicine or from the Nebraska Organ Retrieval System in accordance with the guidelines of the University of Nebraska Institutional Review Board. Current smokers and those with a >20 pack yr history of smoking, known lung disease, lung infection, or sepsis were excluded. HLF were isolated using an established protocol (1). Briefly, peripheral lung parenchyma was minced with a scalpel (2–3 mm pieces) in 100 mm dishes in DMEM (Cellgro, Corning, Manassas, VA) containing 10% FBS and antibiotics (pen-strep, Hyclone, South Logan, Utah). Culture plates were maintained in a 37°C incubator at 5% CO_2 to allow outgrowth of fibroblasts. Cells were passaged using TrypLE Express (Life Technologies, Carlsbad, CA), and passaged cultures included only negligible contaminating cell types. Fibroblasts used in these experiments were passaged not more than four times. Cells from three separate mice and four different human donors were used in these experiments. Levels of IL-6, murine CXCL1, or human IL-8 (neutrophil chemoattractants) and AREG of cell-free supernates of fibroblasts cultured with and without 5% DE

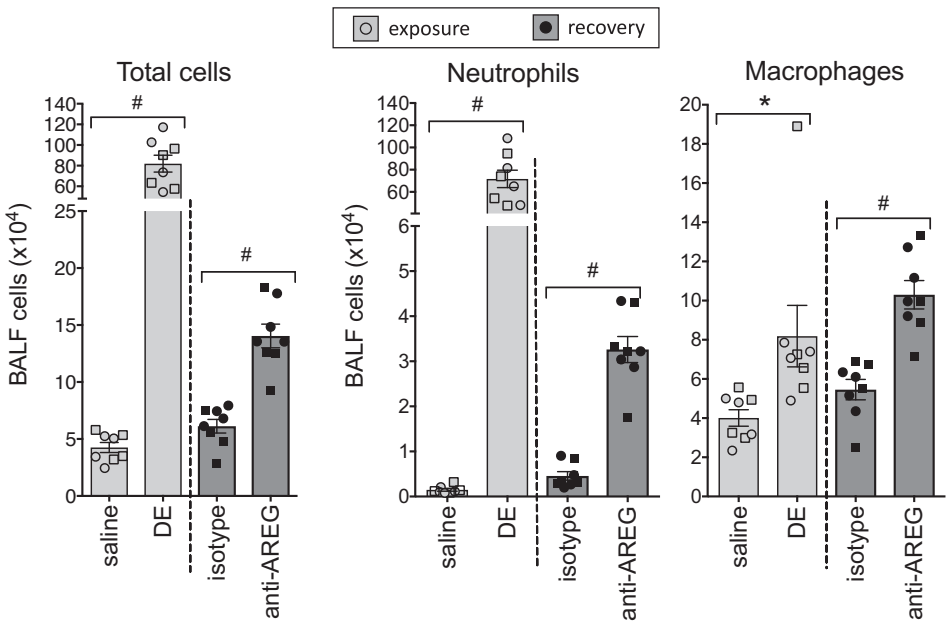

Fig. 2. Inhibition of amphiregulin (AREG) impairs recovery from dust extract (DE)-induced inflammatory cell influx. Bronchoalveolar lavage fluid (BALF) cells, neutrophils, and macrophages were markedly elevated in mice repetitively exposed to intranasal DE compared with saline-treated mice. Mice treated with anti-AREG antibody during and after DE challenge demonstrated an impaired recovery response compared with mice given an isotype control antibody. No significant differences were observed between male (circles) and female (squares) responses. *$P < 0.05$, #$P < 0.01$, by ANOVA.

for 2, 6, 12, and 24 h were determined by murine or human-specific ELISA, as previously described (23).

Quantitative real-time PCR. Primary murine and human fibroblasts were plated on uncoated six-well tissue culture plates and grown to 90% confluency in HLF growth medium. Cells were treated with 5% DE or medium alone for 2, 6, or 24 h, after which cells were gently dissociated from the plates (TrypLE Express, Life Technologies), pelleted, and flash frozen for mRNA extraction. mRNA extraction was performed using the RNeasy Mini Kit (Qiagen, Germantown, MD) according to the manufacturer's instructions. The quantity of mRNA was spectrophotometrically measured. Total cDNA was prepared using the Taqman real-time PCR kit (Applied Biosystems, Foster City, CA) according to the manufacturer's instructions using 100 ng of RNA template and 2.5 μM random hexamers. The real-time PCR reaction mixture consisted of a cocktail of Taqman universal Master Mix (Applied Biosystems), primers for murine *AREG* (Applied Biosystems Mm00437583) and human *AREG* (Applied Biosystems Hs00152928), and the endogenous control gene 18S ribosomal RNA (Applied Biosystems). Reactions were performed in duplicate. Real-time PCR was performed using an ABI Prism 7500 sequence detection system (Applied Biosystems). The PCR conditions were 2 min at 50°C and 10 min at 95°C, followed by 40 cycles of 15 s at 95°C and 1 min at 60°C. *AREG* was normalized to the housekeeping gene 18S ribosomal RNA using the ΔΔCT method (41). Data are reported as fold change compared with time-matched saline control.

Decellularized lung scaffold model. Normal human lungs deemed unsuitable for transplant were obtained from tissue repositories (International Institute for the Advancement of Medicine, Nebraska Organ Retrieval System, as above) and processed as previously reported (23). Briefly, lung lobes were carefully dissected and decellularized by serial detergent washes (0.1% Triton X-100, 48 h, H_2O rinse, 2% sodium deoxycholate twice, 48 h each, DNase, 2 h, H_2O rinse). Decellularized lung lobes were then inflated with warm 2% low melting point agarose (melting point: 37°C, Low EEO, Fisher Scientific) and allowed to solidify at 4°C. Tissue cores were made with a 10-mm-diameter biopsy punch, and 300-μm-thick sections were prepared using a vibratome (Compresstome, Precisionary Instruments, Greenville, NC). The resulting disks of lung tissue (scaffolds) were stored in a 30% ethanol/PBS solution at −20°C until use. Following this procedure, virtually all cellular components were eliminated from the mesenchymal matrix. For experiments, scaffolds were rinsed twice in PBS and equilibrated in HLF culture medium at 37°C before being placed into 12-well dishes and seeded with fibroblasts. Immediately after 1×10^5 HLF were seeded on each scaffold matrix, scaffold cultures were treated with 5% DE, 10 ng/mL recombinant human AREG (R&D Systems, 262-AR), and 0.5 μg/mL of an AREG-neutralizing antibody (R&D Systems, AF262), an isotype control antibody (0.5 μg/mL rabbit IgG, Abcam, Cambridge, MA), or the combination of DE + AREG in HLF growth medium. Cultures were refed with the above conditions every second day, and on *day 5*,

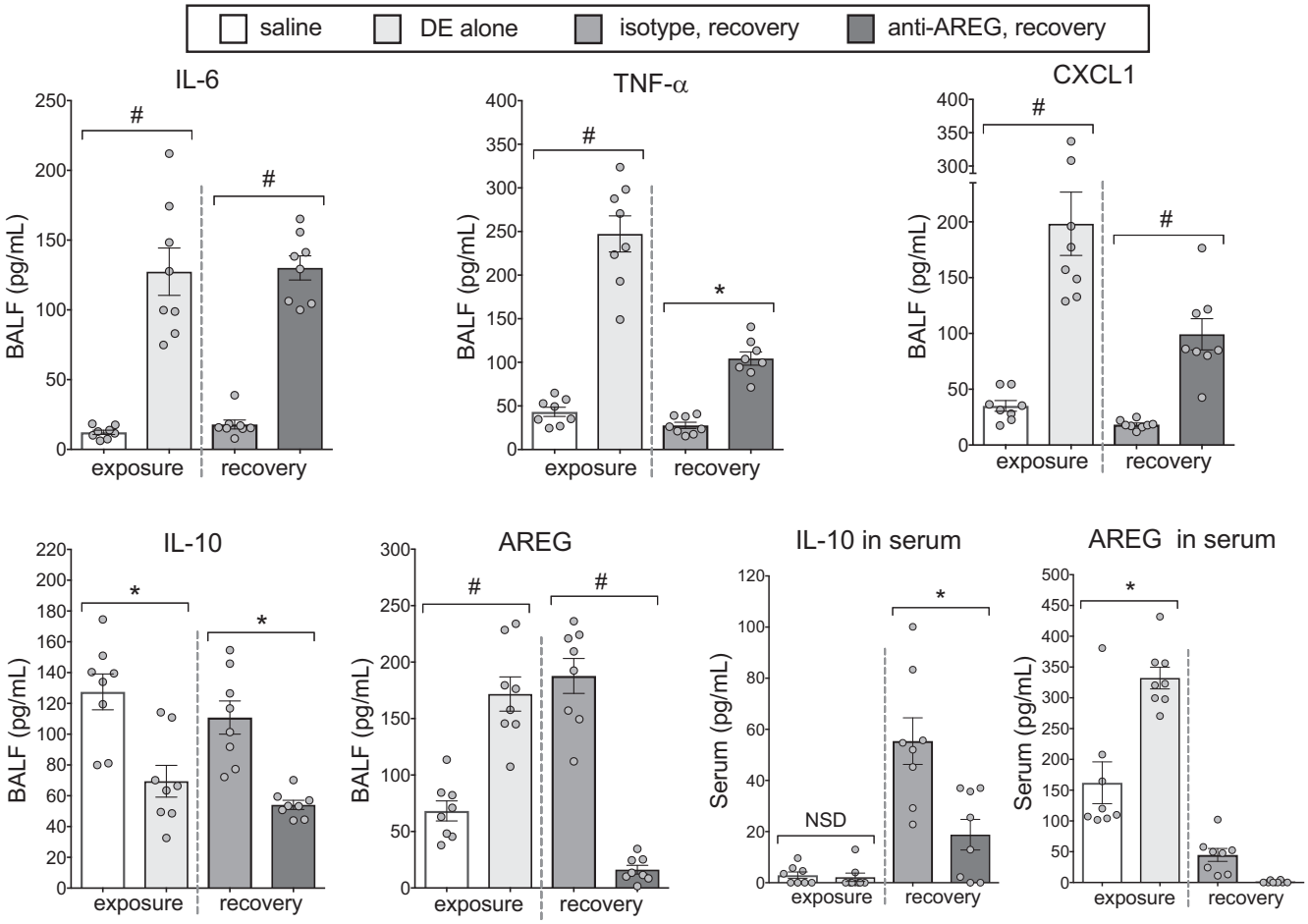

Fig. 3. Amphirgeulin (AREG) blockade impedes the normal attenuation of dust extract (DE)-mediated inflammation during recovery. DE-challenged mice demonstrated significantly elevated proinflammatory cytokines (IL-6, TNF, CXCL1) and AREG and reduced IL-10 in bronchoalveolar lavage fluid (BALF) compared with saline-treated mice (exposure). Inflammatory cytokine levels fell dramatically during the recovery phase in isotype-treated mice, but in mice given AREG antibody, relatively high cytokine levels persisted (recovery). DE-induced IL-10 and AREG levels remained elevated after recovery for isotype groups but were reduced in anti-AREG groups. Serum levels of IL-10 increased in isotype-treated mice during recovery, whereas AREG blockade blunted this response (*inset*). AREG was not detected in serum from mice treated with anti-AREG antibody. *$P < 0.05$; #$P < 0.01$, by ANOVA. NSD, no significant difference.

scaffold disks were transferred to fresh culture dishes, and cell numbers were determined using a commercially available proliferation kit (Vybrant MTT cell proliferation assay, Thermo Fisher). Results from four independent experiments are reported.

Wound repair assays. Primary murine and human fibroblasts were grown to confluence on standard uncoated tissue culture cluster plates. Circular wounds were made using a modified sterile nylon inoculation loop in the center of each well. Cell layers were rinsed once with growth medium, refed with serum-free DMEM, and photographed (baseline wound area). Wounded monolayers were then treated with medium alone, 5% DE, 10 ng/mL recombinant murine or human AREG, or the combination of DE + AREG. After 6, 18, and 24 h, the wound area of each well was analyzed using NIH ImageJ image analysis software and compared with initial wound area (T_0). Alternatively, monolayers were treated with an AREG-neutralizing antibody or isotype control antibody (each at 0.5 μg/mL) and monitored for wound closure as above.

Statistical methods. Data are presented as the mean ± SE where indicated. To detect significant changes between two groups, statistics were performed using a nonparametric, two-tailed Mann–Whitney test. For experiments with three or more groups, one-way analysis of variance (ANOVA) was used with Tukey's post hoc test for multiple comparisons within groups. Statistical analysis was performed using GraphPad Prism software (La Jolla, CA) and/or SPSS software (SPSS, Chicago, IL), and significance was set at $P < 0.05$.

RESULTS

AREG blockade impedes the normal recovery of DE-mediated airway inflammatory response. Mice ($n = 8$ per treatment group) challenged with repeated DE exposure over 8 days demonstrated a significant ($P < 0.05$) influx in total cells, macrophages, and neutrophils in the BAL fluid compared with saline-treated mice (Fig. 2). Mice treated with AREG-neutralizing antibody during and after DE exposure demonstrated an impaired recovery response. Specifically, the number of airway total cells, neutrophils, and macrophages was significantly ($P < 0.01$) increased in anti-AREG antibody-treated mice compared with isotype control antibody-treated animals (Fig. 2). There was no difference between male and female mice for any of the experimental end points.

Repeated DE exposure increased the levels of the proinflammatory cytokines IL-6, TNF-α, and CXCL1 compared with saline, and mice treated with anti-AREG antibody before and during recovery from DE exposure demonstrated increased levels of IL-6, TNF-α, and CXCL1 compared with animals treated with isotype control antibody (Fig. 3). AREG levels in BAL fluid were significantly increased with repeated DE exposure, and these levels remained elevated in mice treated with isotype control antibody but significantly reduced with AREG blockade. Interestingly, the anti-inflammatory cytokine IL-10 was significantly reduced in mice repetitively treated with DE, and moreover, IL-10 levels recovered with isotype control antibody treatment (saline vs. isotype control antibody, $P = 0.61$) but not anti-AREG antibody treatment. Differences in serum IL-10 and AREG were also demonstrated. Although there was no difference in serum IL-10 levels between saline and DE exposure, serum IL-10 was elevated in the recovery phase, and this response was significantly blunted in anti-AREG-treated mice compared with control antibody-treated mice. Serum AREG levels were increased in DE-exposed

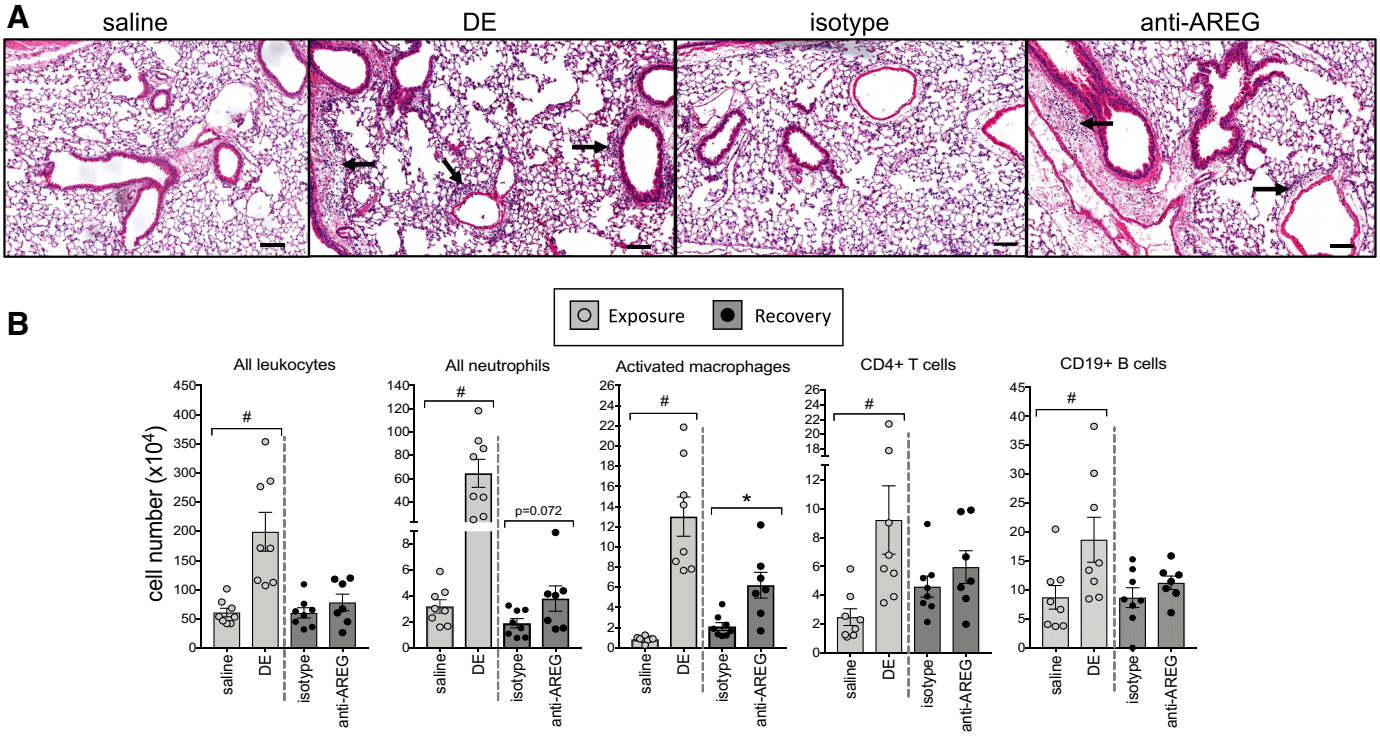

Fig. 4. Amphiregulin is important for clearance of inflammatory effector cells during recovery. A representative hematoxylin and eosin-stained lung section (4–5 μm) from each treatment group is shown at ×10 magnification with line scale at 100 μm (*A*). Arrows indicate perivascular and peribronchiolar cellular infiltrates. To quantitate changes, immune effector cells in dissociated lung tissue were analyzed by flow cytometry (*B*). Number of total leukocytes, neutrophils ($Ly6G^+$), activated macrophages ($CD11c^{hi}CD11b^{hi}$), $CD3^+CD4^+$ T cells, and $CD3^-CD19^+$ B cells from mice exposed to repetitive dust extract (DE) were strikingly elevated compared with saline-treated mice. Mice injected with isotype control antibody before and during the recovery phase effectively cleared immune cells, whereas mice treated with anti-amphiregulin (AREG) displayed a defective clearance function. $*P < 0.05$; $\#P < 0.01$, by Mann–Whitney test.

animals, and AREG was not detected in the serum of anti-AREG-treated mice (Fig. 3, inset box).

Note that there were no significant differences ($P > 0.05$) in DE-induced total cell, neutrophil, macrophage, and lymphocyte influx or levels of IL-6, TNF-α, CXCL1, and IL-10 in BALF between mice treated with isotype control antibody and mice treated with anti-AREG over the 8 days of exposure despite a reduction in AREG levels ($P = 0.0019$) (Supplemental Fig. S1; Supplemental Material is available at http://dx.doi.org/10.17632/fmv39wsywy.2). Collectively, these data support a role for AREG in recovery but not induction of airway inflammation.

AREG impacts lung infiltrates of DE-induced inflammatory effector cells during recovery. By microscopic review, repeated dust exposure induced lung cell perivascular and peribronchiolar cellular infiltrates that were reduced in recovery (Fig. 4*A*). To quantitate changes among groups, lung cell infiltrates isolated from homogenized whole lungs were phenotyped by flow cytometry, as described in the METHODS section. Total lung leukocytes, neutrophils, $CD11c^+CD11b^{hi}$ exudative macrophages, $CD4^+$ T cells, and $CD19^+$ B cells were increased in mice exposed to DE compared with saline control (Fig. 4*B*). Lung inflammatory effector cells were reduced during recovery regardless of antibody treatment, with the exception that the exudative/activated $CD11c^+CD11b^{hi}$ macrophages were significantly increased ($P < 0.05$) in anti-AREG-treated mice compared with isotype control mice. During recovery, a trend ($P = 0.072$) toward the persistence of tissue neutrophils in the anti-AREG treatment group was also observed. There were no differences among treatment groups in alveolar $CD11c^+CD11b^{lo}$ macrophages and $CD8^+$ T cells (data not shown). Collectively, these murine studies indicate that blocking AREG before and during recovery from repeated DE exposure prevents normative recovery and suggest that AREG plays a role in lung repair mechanisms.

Murine and human lung fibroblasts are responsive to DE stimulation and release AREG. In the following experiments, primary MLF and HLF were utilized to elucidate the potential role for fibroblasts in the context of DE-induced inflammation and AREG-mediated repair. First, we sought to determine whether DE would induce proinflammatory cytokine release as well as AREG protein and gene expression. DE challenge induced AREG mRNA in MLF (3 independent experiments; 12 technical replications) at 6 h postexposure (~150-fold increase over 6 h control groups) as determined by quantitative RT-PCR, with this upregulation attenuated by 24 h (Fig. 5*A*).

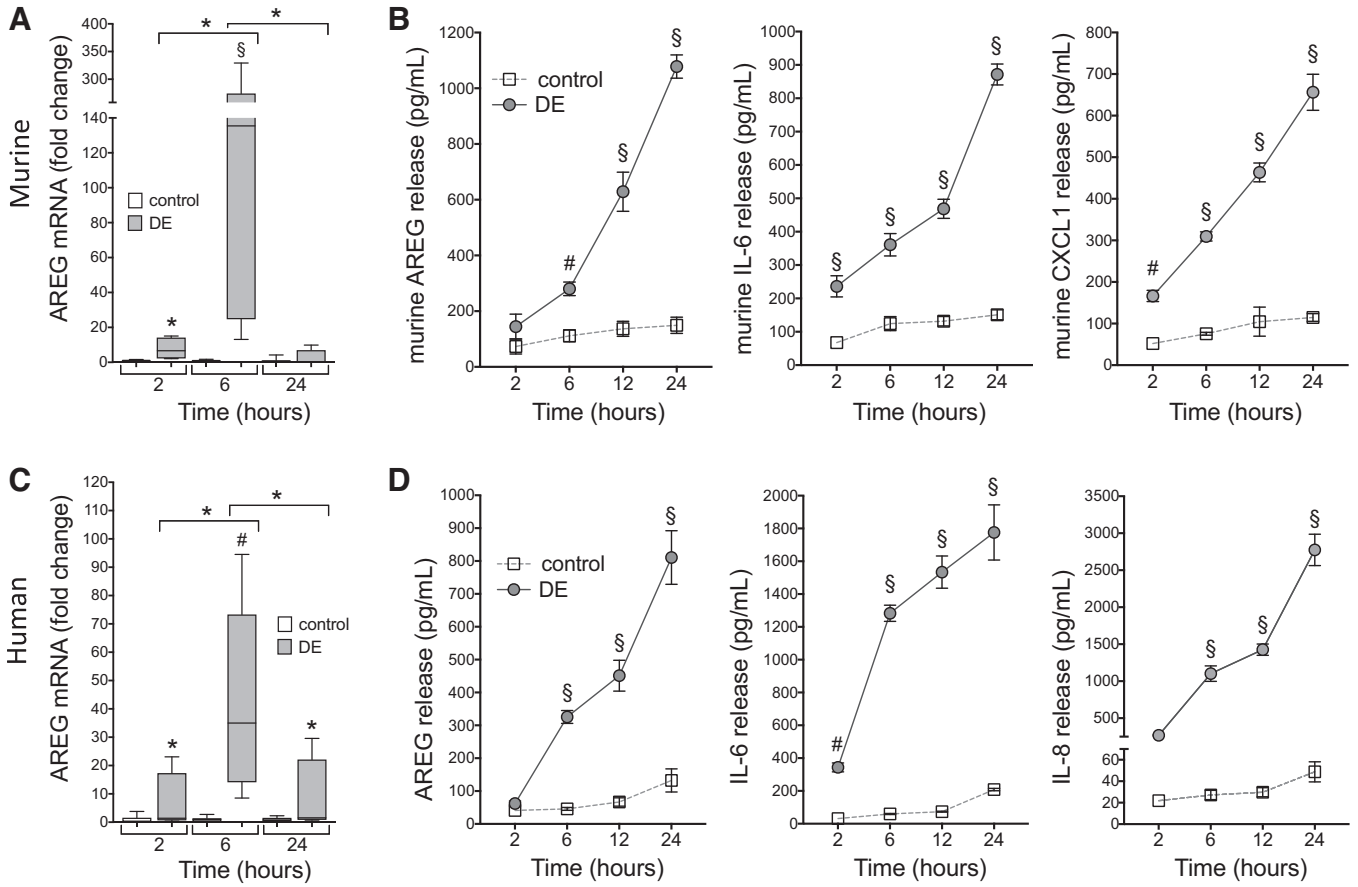

Fig. 5. Dust extract (DE) stimulates amphiregulin (AREG) mRNA and immune modulator release in primary fibroblasts in culture. Primary murine lung fibroblasts (MLF) and human lung fibroblasts (HLF) were treated with 5% DE or medium alone (control) for 2–24 h. Murine (*A*) and human (*C*) *AREG* gene expression were measured by quantitative real-time PCR in lysates at 2, 6, and 24 h. Fold change in *AREG* message normalized to ribosomal compared with corresponding control time is shown. Three independent experiments were performed for MLF and HLF using different cell isolates. Boxplots for *AREG* message indicate medians and quartiles for 12 technical replicates for each condition. Inflammatory mediators murine AREG, IL-6, and CXCL1 (*B*) and human AREG, IL-6, and IL-8 (*D*) were measured in supernates at indicated time points. Data shown are means ± SE for four independent experiments ($n = 24$ technical replicates per condition for *B* and *D*). *$P < 0.05$, #$P < 0.01$, §$P < 0.001$ vs. control at corresponding time points, by ANOVA.

Likewise, stimulation of cultured MLF with DE resulted in prominent increases in IL-6 and the murine IL-8 cognate CXCL1 release over time (Fig. 5*B*). Release of the repair mediator, AREG, was also increased in a time-dependent fashion following DE (Fig. 5*B*). In parallel experiments using human fibroblasts isolated from four different donors, similar results were observed. Namely, there was a significant increase of DE-induced *AREG* gene expression at 6 h postexposure (~43-fold increase over 6 h control groups) (Fig. 5*C*) with increases in DE-induced IL-6, IL-8, and AREG over time (12 technical replicates per condition; Fig. 5*D*).

DE inhibits and AREG promotes fibroblast recellularization of human lung scaffold matrixes. To assess lung wound repair process, we utilized a three-dimensional ex vivo decellularized human lung scaffold model. We have previously demonstrated that primary human bronchial epithelial cells can engraft and recellularize this scaffold matrix (23), and here, we demonstrate fibroblast engraftment and recellularization on lung scaffold matrixes at 5 days in culture (Fig. 6*A*). Using this technique, DE exposure inhibited, but AREG treatment promoted, recellularization of the scaffold cultures as assessed by formazan crystal formation in an MTT assay after 5 days. AREG treatment partially reversed the adverse effects of DE on recellularization (Fig. 6*B*). Four independent experiments were conducted; $n = 16$ scaffold cultures per condition.

DE inhibits and AREG dose responsively accelerates fibroblast wound closure. Wound repair processes involving fibroblast proliferation and/or migration were also assessed using a standard wound closure model whereby primary murine and human fibroblasts were treated with DE, AREG, or anti-AREG antibody after circular wounds were created in confluent cell cultures. Both MLF and HLF exposed to DE demonstrated impaired wound repair evident by a significant reduction in percent closure of wound area at 6, 18, and 24 h as quantified by NIH Image J software (Fig. 7, *A* and *C*). In contrast, treatment with AREG alone accelerated wound closure at 18 and 24 h post-wounding. When AREG was combined with DE (DE + AREG), wound closure was hastened at all time points in MLF cultures and at 24 h in HLF compared with DE alone ($P < 0.05$; Fig. 7, *A* and *C*). Anti-AREG antibody treatment significantly reduced wound area closure at all time points in MLF cultures and at 24 h in HLF compared with isotype antibody control-treated cells (Fig. 7, *B* and *D*).

Recombinant AREG promotes resolution of DE-induced airway inflammatory response. To assess whether AREG supplementation would be a beneficial approach in the recovery phase following DE-induced exposure, mice were treated in two separate side-by-side studies with rAREG (or saline vehicle control) intranasally for 3 days following DE exposure phase (see overview schematic in Fig. 1*B*; $n = 6$ mice/group, 2 independent studies). There was a significant reduction in DE-induced total cells and neutrophil influx in mice treated with rAREG compared with control in the recovery phase (Fig. 8*A*). As determined by flow cytometry analysis of dissociated lung cells, intranasal rAREG treatment resulted in a reduction in DE-induced total lung leukocytes, neutrophils, and activated ($CD11c^+CD11b^{hi}$) macrophages and an increase in lung $CD8^+$ T cells (Fig. 8*B*). There were no differences in alveolar macrophages, CD4+ T cells, or B cells between treatment groups (data not shown). Likewise, there were significant reductions in DE-induced BALF IL-6, TNF-α, and CXCL1 following rAREG treatment, corresponding to significant increases in levels of the prorepair mediators AREG and IL-10 (Fig. 8*C*). AREG supplementation during recovery also induced IL-10 release and AREG levels in serum (Fig. 8*D*). This concentration of rAREG (1 μg) daily for 3 days does not elicit neutrophil influx or inflammatory cytokine release but does increase serum and lavage fluid AREG levels compared with saline control (Supplemental Fig. S2, http://dx.doi.org/10.17632/fmv39wsywy.2).

DISCUSSION

Exposure to aerosolized dust in agricultural environments causes airway inflammatory diseases, including chronic bron-

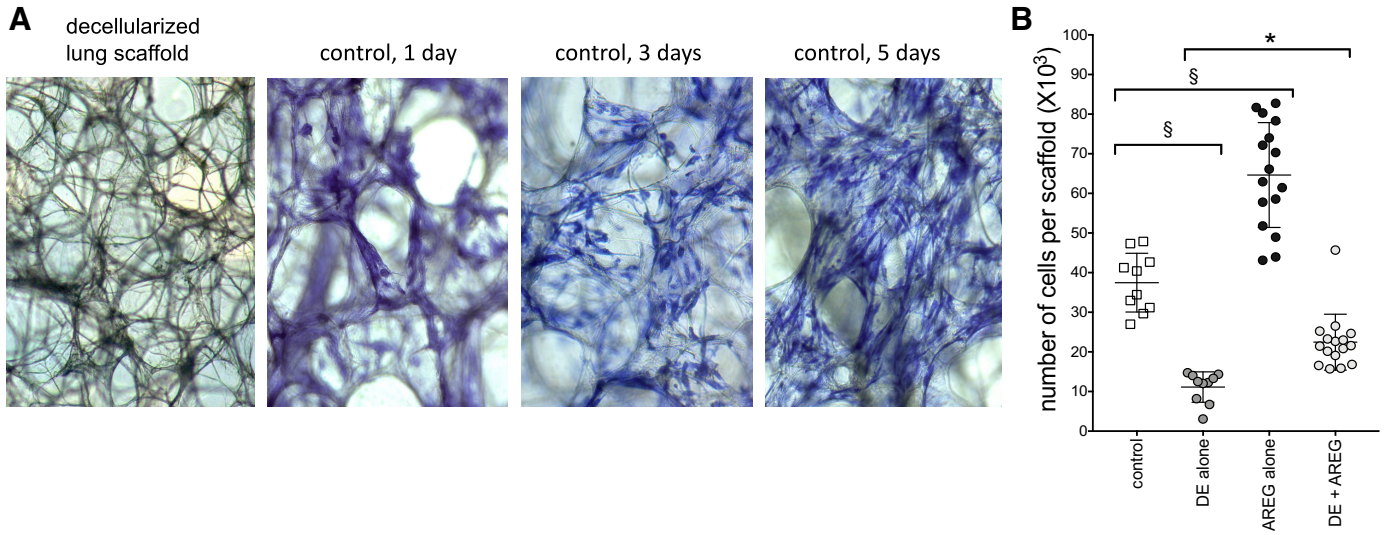

Fig. 6. Dust extract (DE) inhibits and amphiregulin (AREG) promotes recellularization of human lung scaffold matrixes by human lung fibroblasts (HLF). Denuded human lung mesenchymal scaffolds were seeded with human primary lung fibroblasts and cultured for 5 days (*A*). Scaffold cultures were treated with medium alone (control), DE, and/or AREG on *day 1*. Recellularization of the scaffold cultures was assessed by MTT uptake and formazan crystal formation on *day 5* (*B*). Each symbol represents one scaffold culture ($n = 16$ scaffolds per condition). *$P < 0.05$; §$P < 0.001$, by ANOVA.

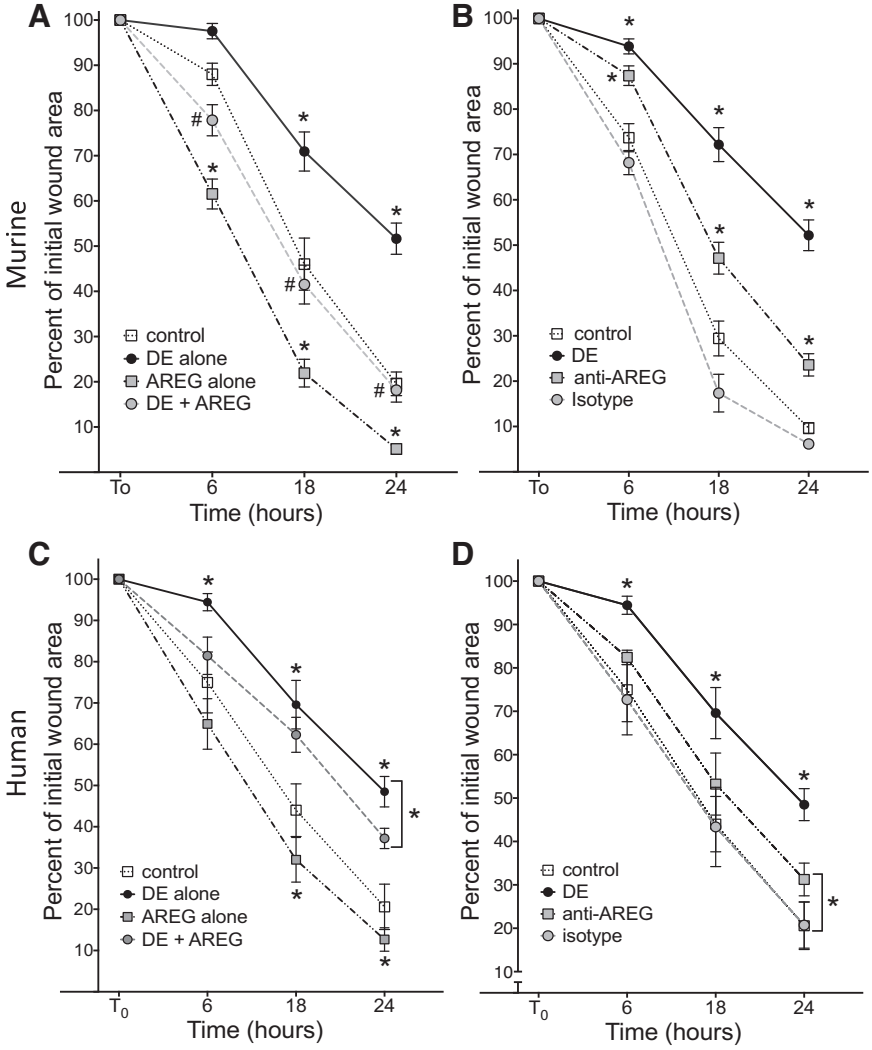

Fig. 7. Amphiregulin signaling modulates dust extract (DE)-induced fibroblast wound repair. A circular wound was made in confluent murine lung fibroblast (MLF) (*A*) or human lung fibroblast (HLF) (*C*) monolayers, and wells were then treated with medium alone, 5% DE alone, amphiregulin (AREG) alone, or DE + AREG. Alternatively, cells were wounded in the presence of anti-AREG or isotype control antibody (*B* and *D*). After 6, 18, and 24 h, the size of the wound area was quantified by image analysis and compared with initial wound areas. Results shown are mean measurements for four independent experiments ($n = 16$ biological replicates). *$P < 0.05$ vs. corresponding control time points or indicated comparisons, #$P < 0.05$ vs. DE, by ANOVA.

chitis and obstructive pulmonary disease (10). No treatments currently exist to significantly reverse exposure-induced respiratory disease because of an incomplete knowledge of the processes governing the transition from environmental dust-induced airway inflammation to repair and recovery. We previously demonstrated that AREG is released from DE-stimulated bronchial epithelial cells and that blocking AREG reduced epithelial recellularization of lung scaffolds (23). We have also reported that AREG is increasingly released in BALF over 4 wk of recovery time following repetitive DE exposure in mice (48). We interpreted these findings to suggest a role for AREG in modulating repair and recovery processes following organic dust exposures. Because others have characterized AREG as both protective and injurious in the progression of various other lung diseases (2, 13, 18, 37), our primary objective in this current study was to define whether targeting AREG in an animal model would impact lung recovery following repeated DE exposures.

In published murine studies, organic dust exposures elicit neutrophil influx with corresponding increases in proinflammatory cytokines and neutrophil chemokines that rapidly abate once exposure is removed (27, 48). Therefore, our first strategy was to block AREG through the use of an anti-AREG-neutralizing antibody administered before and during recovery with the hypothesis that this would prevent normative recovery. Repeated exposure to DE induced a strong inflammatory cellular and mediator response detected in the lavage fluid, and this response was cleared after 6 days of no exposure (recovery) in the control antibody-treated animals. Blocking AREG strikingly blunted this normative recovery response. Moreover, mice treated with control antibody demonstrated significant resolution of the inflammatory response and exhibited increased airway AREG and anti-inflammatory IL-10 along with increased systemic IL-10 levels in contrast to the anti-AREG-treated animals. Blocking AREG during only the exposure phase of DE-induced inflammation did not significantly alter airway inflammatory responses, but blocking AREG during exposure and recovery resulted in an increase in airway inflammatory parameters demonstrated at 1 wk post-recovery. However, it remains possible that the post-recovery effect of blocking AREG was initiated during the exposure phase. Thus, these data suggest that AREG functions to promote resolution of dust-induced inflammation by promoting anti-inflammatory processes during recovery from an environmental insult. Others have shown that in the setting of lung and gastric cancers, elevated levels of AREG increase suppressive T cell regulatory

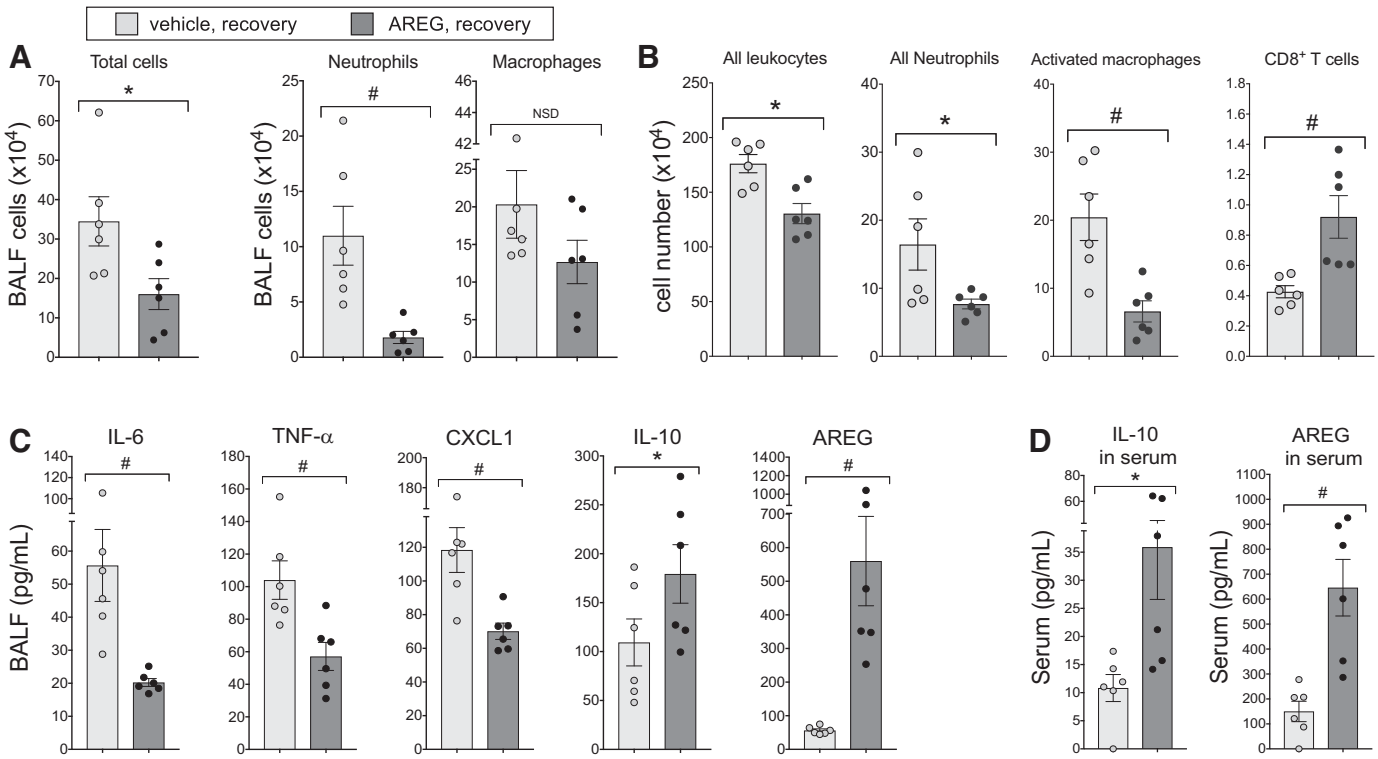

Fig. 8. Amphiregulin (AREG) supplementation promotes recovery following inflammatory assault. Mice given intranasal recombinant AREG during 3 days of recovery following 8 days of dust extract (DE) exposure exhibited fewer inflammatory cell infiltrates than control mice (*A*), and inflammatory cell subsets in dissociated whole lung were influenced by AREG treatment (total leukocytes, neutrophils, and activated macrophages significantly suppressed, but T cells elevated) (*B*). Proinflammatory modulators in bronchoalveolar lavage fluid (BALF) were uniformly attenuated in AREG-treated groups, whereas prorepair proteins IL-10 and AREG were augmented, compared with vehicle (*C*). Administration of AREG during recovery also stimulated significantly higher levels of IL-10 and AREG in serum (*D*). $*P < 0.05$, $\#P < 0.01$. NSD, no significant difference.

function through post-translational regulation of Foxp3 expression (47). The impact of blocking AREG in our studies did not impact T or B cell numbers, but future studies could investigate whether there is a role for AREG in adaptive immune responses in either longer DE exposure models or at earlier time points during the recovery period.

Classically activated or exudative $CD11c^+CD11b^{hi}$ macrophages are upregulated at 3–5 wk of repetitive organic dust exposures (29, 38), and here, we found this response to occur after six repeated DE challenges given over 8 days. Moreover, these cells remained elevated with anti-AREG treatment following recovery from DE exposure, implicating AREG in regulating this macrophage phenotype. Classically activated lung macrophages play an important role in response to lung inflammation and in the recovery process. In bleomycin-induced pulmonary fibrosis, adoptive transfer of bone marrow-derived $CD11c^+$ cells from bleomycin-treated donor mice exacerbated lung fibrosis, but not if the donor cells were made AREG deficient before transfer (8). This was interpreted to suggest that AREG production induced by bleomycin exposure in recruited $CD11c^+$ cells promoted pulmonary fibrosis, but the role of these AREG-deficient cells after the inflammatory stimulus (bleomycin) is removed is not known. In the setting of environmental dust exposure, it has been shown that depletion of lung macrophages resulted in an augmented lung inflammatory response (29). In the current study, the continued presence of tissue-resident lung $CD11c^+CD11b^{hi}$ macrophages with trends toward increased lung neutrophils coincident with AREG blockade suggests the persistence of lung inflammation after systemic inhibition of AREG. However, the inflammatory responses in the lung tissue were overall modest, which might reflect the duration of exposure or could indicate a compartmentalized response with the role of AREG most prominent in the airspaces.

Because blocking AREG resulted in an impairment in lung repair/recovery from DE in vivo, we sought to investigate the contribution of fibroblasts to this process because of their recognized role in mediating repair. First, we demonstrated that murine and human fibroblasts are responsive to DE. DE stimulated IL-6 and IL-8 release, reduced the ability of fibroblasts to recellularize human lung scaffold matrixes, and inhibited fibroblast wound closure. These findings indicate that agricultural DE exposures reduce fibroblast function that could impair lung repair and recovery processes. We also found that DE induced AREG gene expression and protein release from MLF and HLF. This observation is important because lung fibroblasts have not been previously recognized as a significant cellular source of AREG, which is predominantly attributed to epithelial cells and macrophages in the lung (2, 8). Future studies could investigate the relative contribution of lung fibroblast-derived AREG in vivo.

Recombinant AREG treatment alone enhanced fibroblast recellularization on human lung scaffold matrixes and promoted wound repair, which is consistent with other reports establishing that AREG elicited fibroblast proliferation and migration (2). In contrast, blocking AREG (anti-AREG

antibody treatment) resulted in a reduction of fibroblast wound closure, but there was no significant difference in lung scaffold recellularization with anti-AREG and isotype antibody (data not shown). More importantly, we demonstrated that recombinant AREG treatment reversed the adverse effects induced by DE by promoting recellularization of scaffolds and wound closure. Recombinant AREG administration has also been shown to reverse DE-mediated epithelial cell dysregulation (23).

Thus, clinical strategies in humans to augment, as opposed to neutralize, lung AREG might be warranted to reduce inflammatory disease and/or promote repair and recovery. In this current study, we demonstrated that, indeed, delivery of rAREG to the lung via intranasal inhalation method after DE exposure had ceased hastened resolution of DE-induced airway inflammatory responses. This was marked by reduction in neutrophils, proinflammatory cytokines, and activated macrophages. Interestingly, this response corresponded with increases in IL-10, further supporting a link between AREG and IL-10. As found with the AREG neutralization strategies, intranasal inhalation of rAREG also did not affect airway inflammation when given only during DE exposure (data not shown). Careful attention to this strategic approach in humans would be required because the presence of AREG in tumor microenvironments is thought to contribute to therapeutic resistance, and thus, approaches in cancer biology have focused on blocking AREG (54). Similarly, exogenous AREG from programmed macrophages promotes lung fibrosis (8). However, administration of AREG has been reported to reduce infection-induced skeletal muscle inflammation and damage by promoting repair and resolution mechanisms (15). Although there was not a clear adverse reaction observed with AREG administration for 3 days, we did see an increase in lung $CD8^+$ T cells. Thus, further studies to fully define potential treatment windows, duration of therapy, delivery methods, and potential adverse interactions are necessary as well as determine the impact of AREG in other environmental inflammatory bioaerosol exposures, including air pollution. These studies are necessary, as chronic delivery of AREG over time could lead to lung fibrosis. Moreover, these approaches, particularly short-term delivery, could lead to important clinical strategies to mitigate postexposure-induced lung disease following natural and/or manmade disasters that generate environmental inflammatory exposures.

In summary, AREG plays an important role in agricultural dust-mediated lung disease, as inhibiting AREG during and after exposure repeated dust extract exposures prevented the normative lung repair and recovery process, whereas intranasal AREG supplementation for 3 days during only the recovery process demonstrated beneficial responses. Organic dust exposure also impacts lung fibroblasts through a reduction in recellularization and wound closure functional properties that can be rescued with exogenous AREG treatment. Targeting AREG pathways in bioaerosol-exposed persons might represent a novel approach to disease management.

ACKNOWLEDGMENTS

The authors thank members of the Tissue Sciences Facility at the Department of Pathology and Microbiology Department (University of Nebraska Medical Center) for assistance with lung tissue processing, sectioning, and hematoxylin and eosin staining and assistance with digital microscopy images prepared for the manuscript. We thank members of the Flow Cytometry Research Core Facility at the University of Nebraska Medical Center for providing assistance with flow cytometry. We thank Lisa Chudomelka for editorial assistance and manuscript submission.

GRANTS

This study was supported by the National Institute of Occupational Safety and Health (NIOSH, RO1:OH008539-09 and Veterans Affairs Merit Review 1-I01 CX001714-01A1 to D. J. Romberger). This study was supported by grants from the National Institute of Environmental Health Sciences (R01: ES019325 to J. A. Poole; R00-ES025819 to T. M. Nordgren) and the National Institute of Occupational Safety and Health (U54OH010162 to J. A. Poole). This study was also supported by the Fred & Pamela Buffett Cancer Center (Flow Cytometry Research Facility and Tissue Sciences Facility) Shared Resource, supported by the National Cancer Institute under award number P30 CA 36727.

DISCLOSURES

No conflicts of interest, financial or otherwise, are declared by the authors.

AUTHOR CONTRIBUTIONS

J.A.P., T.M.N., D.K., K.L.B., and D.J.R. conceived and designed research; J.A.P., T.M.N., A.J.H., A.J.N., D.K., and K.L.B. performed experiments; J.A.P., T.M.N., A.J.H., D.K., K.L.B., and D.J.R. analyzed data; J.A.P., T.M.N., and D.J.R. interpreted results of experiments; J.A.P., T.M.N., A.J.H., and A.J.N. prepared figures; J.A.P. and T.M.N. drafted manuscript; J.A.P., T.M.N., A.J.H., A.J.N., D.K., K.L.B., and D.J.R. edited and revised manuscript; J.A.P., T.M.N., A.J.H., A.J.N., D.K., K.L.B., and D.J.R. approved final version of manuscript.

REFERENCES

1. **Bailey KL, Robinson JE, Sisson JH, Wyatt TA.** Alcohol decreases RhoA activity through a nitric oxide (NO)/cyclic GMP(cGMP)/protein kinase G (PKG)-dependent pathway in the airway epithelium. *Alcohol Clin Exp Res* 35: 1277–1281, 2011. doi:10.1111/j.1530-0277.2011.01463.x.
2. **Berasain C, Avila MA.** Amphiregulin. *Semin Cell Dev Biol* 28: 31–41, 2014. doi:10.1016/j.semcdb.2014.01.005.
3. **Boissy RJ, Romberger DJ, Roughead WA, Weissenburger-Moser L, Poole JA, Levan TD.** Shotgun pyrosequencing metagenomic analyses of dusts from swine confinement and grain facilities. *PLoS One* 9: e95578, 2014. doi:10.1371/journal.pone.0095578.
4. **Boucherat O, Morissette MC, Provencher S, Bonnet S, Maltais F.** Bridging lung development with chronic obstructive pulmonary disease. Relevance of developmental pathways in chronic obstructive pulmonary disease pathogenesis. *Am J Respir Crit Care Med* 193: 362–375, 2016. doi:10.1164/rccm.201508-1518PP.
5. **Burgel PR, Nadel JA.** Epidermal growth factor receptor-mediated innate immune responses and their roles in airway diseases. *Eur Respir J* 32: 1068–1081, 2008. doi:10.1183/09031936.00172007.
6. **Burke JP, Cunningham MF, Watson RW, Docherty NG, Coffey JC, O'Connell PR.** Bacterial lipopolysaccharide promotes profibrotic activation of intestinal fibroblasts. *Br J Surg* 97: 1126–1134, 2010. doi:10.1002/bjs.7045.
7. **Charavaryamath C, Juneau V, Suri SS, Janardhan KS, Townsend H, Singh B.** Role of toll-like receptor 4 in lung inflammation following exposure to swine barn air. 34: 19–35, 2008. doi:10.1080/01902140701807779.
8. **Ding L, Liu T, Wu Z, Hu B, Nakashima T, Ullenbruch M, Gonzalez De Los Santos F, Phan SH.** Bone marrow CD11c+ cell-derived amphiregulin promotes pulmonary fibrosis. *J Immunol* 197: 303–312, 2016. doi:10.4049/jimmunol.1502479.
9. **Dodmane PR, Schulte NA, Heires AJ, Band H, Romberger DJ, Toews ML.** Airway epithelial epidermal growth factor receptor mediates hogbarn dust-induced cytokine release but not Ca2+ response. *Am J Respir Cell Mol Biol* 45: 882–888, 2011. doi:10.1165/rcmb.2010-0419OC.
10. **Eduard W, Pearce N, Douwes J.** Chronic bronchitis, COPD, and lung function in farmers: the role of biological agents. *Chest* 136: 716–725, 2009. doi:10.1378/chest.08-2192.
11. **Gao Z, Dosman JA, Rennie DC, Schwartz DA, Yang IV, Beach J, Senthilselvan A.** Association of toll-like receptor 2 gene polymorphisms with lung function in workers in swine operations. *Ann Allergy Asthma Immunol* 110: 44–50.e1, 2013. doi:10.1016/j.anai.2012.11.003.

12. **Guerrero A, Darszon A.** Egg jelly triggers a calcium influx which inactivates and is inhibited by calmodulin antagonists in the sea urchin sperm. *Biochim Biophys Acta* 980: 109–116, 1989. doi:10.1016/0005-2736(89)90206-X.
13. **Hall OJ, Limjunyawong N, Vermillion MS, Robinson DP, Wohlgemuth N, Pekosz A, Mitzner W, Klein SL.** Progesterone-based therapy protects against influenza by promoting lung repair and recovery in females. *PLoS Pathog* 12: e1005840, 2016. doi:10.1371/journal.ppat.1005840.
14. **Jaffar J, Yang SH, Kim SY, Kim HW, Faiz A, Chrzanowski W, Burgess JK.** Greater cellular stiffness in fibroblasts from patients with idiopathic pulmonary fibrosis. *Am J Physiol Lung Cell Mol Physiol* 315: L59–L65, 2018. doi:10.1152/ajplung.00030.2018.
15. **Jin RM, Warunek J, Wohlfert EA.** Therapeutic administration of IL-10 and amphiregulin alleviates chronic skeletal muscle inflammation and damage induced by infection. *Immunohorizons* 2: 142–154, 2018. doi:10.4049/immunohorizons.1800024.
16. **Kanaji N, Basma H, Nelson A, Farid M, Sato T, Nakanishi M, Wang X, Michalski J, Li Y, Gunji Y, Feghali-Bostwick C, Liu X, Rennard SI.** Fibroblasts that resist cigarette smoke-induced senescence acquire profibrotic phenotypes. *Am J Physiol Lung Cell Mol Physiol* 307: L364–L373, 2014. doi:10.1152/ajplung.00041.2014.
17. **Kim H, Liu X, Kobayashi T, Kohyama T, Wen FQ, Romberger DJ, Conner H, Gilmour PS, Donaldson K, MacNee W, Rennard SI.** Ultrafine carbon black particles inhibit human lung fibroblast-mediated collagen gel contraction. *Am J Respir Cell Mol Biol* 28: 111–121, 2003. doi:10.1165/rcmb.4796.
18. **Krishnamoorthy N, Burkett PR, Dalli J, Abdulnour RE, Colas R, Ramon S, Phipps RP, Petasis NA, Kuchroo VK, Serhan CN, Levy BD.** Cutting edge: maresin-1 engages regulatory T cells to limit type 2 innate lymphoid cell activation and promote resolution of lung inflammation. *J Immunol* 194: 863–867, 2015. doi:10.4049/jimmunol.1402534.
19. **Ma J, Bishoff B, Mercer RR, Barger M, Schwegler-Berry D, Castranova V.** Role of epithelial-mesenchymal transition (EMT) and fibroblast function in cerium oxide nanoparticles-induced lung fibrosis. *Toxicol Appl Pharmacol* 323: 16–25, 2017. doi:10.1016/j.taap.2017.03.015.
20. **Natarajan K, Meganathan V, Mitchell CT, Boggaram V.** Organic dust induces inflammatory gene expression in lung epithelial cells via ROS-dependent STAT-3 activation. 317: L127–L140, 2019. doi:10.1152/ajplung.00448.2018.
21. **Nehmé B, Gilbert Y, Létourneau V, Forster RJ, Veillette M, Villemur R, Duchaine C.** Culture-independent characterization of archaeal biodiversity in swine confinement building bioaerosols. *Appl Environ Microbiol* 75: 5445–5450, 2009. doi:10.1128/AEM.00726-09.
22. **Nehme B, Létourneau V, Forster RJ, Veillette M, Duchaine C.** Culture-independent approach of the bacterial bioaerosol diversity in the standard swine confinement buildings, and assessment of the seasonal effect. *Environ Microbiol* 10: 665–675, 2008. doi:10.1111/j.1462-2920.2007.01489.x.
23. **Nordgren TM, Heires AJ, Bailey KL, Katafiasz DM, Toews ML, Wichman CS, Romberger DJ.** Docosahexaenoic acid enhances amphiregulin-mediated bronchial epithelial cell repair processes following organic dust exposure. *Am J Physiol Lung Cell Mol Physiol* 314: L421–L431, 2018. doi:10.1152/ajplung.00273.2017.
24. **Parnia S, Hamilton LM, Puddicombe SM, Holgate ST, Frew AJ, Davies DE.** Autocrine ligands of the epithelial growth factor receptor mediate inflammatory responses to diesel exhaust particles. *Respir Res* 15: 22, 2014. doi:10.1186/1465-9921-15-22.
25. **Piepkorn M, Pittelkow MR, Cook PW.** Autocrine regulation of keratinocytes: the emerging role of heparin-binding, epidermal growth factor-related growth factors. *J Invest Dermatol* 111: 715–721, 1998. doi:10.1046/j.1523-1747.1998.00390.x.
26. **Plowman GD, Green JM, McDonald VL, Neubauer MG, Disteche CM, Todaro GJ, Shoyab M.** The amphiregulin gene encodes a novel epidermal growth factor-related protein with tumor-inhibitory activity. *Mol Cell Biol* 10: 1969–1981, 1990. doi:10.1128/MCB.10.5.1969.
27. **Poole JA, Anderson L, Gleason AM, West WW, Romberger DJ, Wyatt TA.** Pattern recognition scavenger receptor A/CD204 regulates airway inflammatory homeostasis following organic dust extract exposures. *J Immunotoxicol* 12: 64–73, 2015. doi:10.3109/1547691X.2014.882449.
28. **Poole JA, Gleason AM, Bauer C, West WW, Alexis N, Reynolds SJ, Romberger DJ, Kielian T.** αβ T cells and a mixed Th1/Th17 response are important in organic dust-induced airway disease. *Ann Allergy Asthma Immunol* 109: 266–273.e2, 2012. doi:10.1016/j.anai.2012.06.015.
29. **Poole JA, Gleason AM, Bauer C, West WW, Alexis N, van Rooijen N, Reynolds SJ, Romberger DJ, Kielian TL.** CD11c(+)/CD11b(+) cells are critical for organic dust-elicited murine lung inflammation. *Am J Respir Cell Mol Biol* 47: 652–659, 2012. doi:10.1165/rcmb.2012-0095OC.
30. **Poole JA, Mikuls TR, Duryee MJ, Warren KJ, Wyatt TA, Nelson AJ, Romberger DJ, West WW, Thiele GM.** A role for B cells in organic dust induced lung inflammation. *Respir Res* 18: 214, 2017. doi:10.1186/s12931-017-0703-x.
31. **Poole JA, Thiele GM, Janike K, Nelson AJ, Duryee MJ, Rentfro K, England BR, Romberger DJ, Carrington JM, Wang D, Swanson BJ, Klassen LW, Mikuls TR.** Combined collagen-induced arthritis and organic dust-induced airway inflammation to model inflammatory lung disease in rheumatoid arthritis. *J Bone Miner Res* 34: 1733–1743, 2019. doi:10.1002/jbmr.3745.
32. **Poole JA, Wyatt TA, Kielian T, Oldenburg P, Gleason AM, Bauer A, Golden G, West WW, Sisson JH, Romberger DJ.** Toll-like receptor 2 regulates organic dust-induced airway inflammation. *Am J Respir Cell Mol Biol* 45: 711–719, 2011. doi:10.1165/rcmb.2010-0427OC.
33. **Poole JA, Wyatt TA, Oldenburg PJ, Elliott MK, West WW, Sisson JH, Von Essen SG, Romberger DJ.** Intranasal organic dust exposure-induced airway adaptation response marked by persistent lung inflammation and pathology in mice. *Am J Physiol Lung Cell Mol Physiol* 296: L1085–L1095, 2009. doi:10.1152/ajplung.90622.2008.
34. **Poole JA, Wyatt TA, Romberger DJ, Staab E, Simet S, Reynolds SJ, Sisson JH, Kielian T.** MyD88 in lung resident cells governs airway inflammatory and pulmonary function responses to organic dust treatment. *Respir Res* 16: 111, 2015. doi:10.1186/s12931-015-0272-9.
35. **Rennard SI.** Chronic obstructive pulmonary disease: linking outcomes and pathobiology of disease modification. *Proc Am Thorac Soc* 3: 276–280, 2006. doi:10.1513/pats.200512-129SF.
36. **Rennard SI, Togo S, Holz O.** Cigarette smoke inhibits alveolar repair: a mechanism for the development of emphysema. *Proc Am Thorac Soc* 3: 703–708, 2006. doi:10.1513/pats.200605-121SF.
37. **Richter A, O'Donnell RA, Powell RM, Sanders MW, Holgate ST, Djukanović R, Davies DE.** Autocrine ligands for the epidermal growth factor receptor mediate interleukin-8 release from bronchial epithelial cells in response to cigarette smoke. *Am J Respir Cell Mol Biol* 27: 85–90, 2002. doi:10.1165/ajrcmb.27.1.4789.
38. **Robbe P, Draijer C, Borg TR, Luinge M, Timens W, Wouters IM, Melgert BN, Hylkema MN.** Distinct macrophage phenotypes in allergic and nonallergic lung inflammation. *Am J Physiol Lung Cell Mol Physiol* 308: L358–L367, 2015. doi:10.1152/ajplung.00341.2014.
39. **Robbe P, Spierenburg EA, Draijer C, Brandsma CA, Telenga E, van Oosterhout AJ, van den Berge M, Luinge M, Melgert BN, Heederik D, Timens W, Wouters IM, Hylkema MN.** Shifted T-cell polarisation after agricultural dust exposure in mice and men. *Thorax* 69: 630–637, 2014. doi:10.1136/thoraxjnl-2013-204295.
40. **Romberger DJ, Heires AJ, Nordgren TM, Souder CP, West W, Liu XD, Poole JA, Toews ML, Wyatt TA.** Proteases in agricultural dust induce lung inflammation through PAR-1 and PAR-2 activation. *Am J Physiol Lung Cell Mol Physiol* 309: L388–L399, 2015. doi:10.1152/ajplung.00025.2015.
41. **Schmittgen TD, Livak KJ.** Analyzing real-time PCR data by the comparative C(T) method. *Nat Protoc* 3: 1101–1108, 2008. doi:10.1038/nprot.2008.73.
42. **Schwartz DA, Landas SK, Lassise DL, Burmeister LF, Hunninghake GW, Merchant JA.** Airway injury in swine confinement workers. 116: 630–635, 1992. doi:10.7326/0003-4819-116-8-630.
43. **Senthilselvan A, Chénard L, Kirychuk S, Predicala B, Schwartz DA, Burch LH, Rennie DC, Willson PJ, Dosman JA.** Gender-related tumor necrosis factor-alpha responses in naïve volunteers with Toll-like receptor 4 polymorphisms exposed in a swine confinement facility. *J Interferon Cytokine Res* 29: 781–790, 2009. doi:10.1089/jir.2009.0002.
44. **Senthilselvan A, Dosman JA, Chenard L, Burch LH, Predicala BZ, Sorowski R, Schneberger D, Hurst T, Kirychuk S, Gerdts V, Cormier Y, Rennie DC, Schwartz DA.** Toll-like receptor 4 variants reduce airway response in human subjects at high endotoxin levels in a swine facility. *J Allergy Clin Immunol* 123: 1034–1040, 2009. doi:10.1016/j.jaci.2009.02.019.
45. **Shapiro SD, Ingenito EP.** The pathogenesis of chronic obstructive pulmonary disease: advances in the past 100 years. *Am J Respir Cell Mol Biol* 32: 367–372, 2005. doi:10.1165/rcmb.F296.

46. **Stolarczyk M, Veit G, Schnúr A, Veltman M, Lukacs GL, Scholte BJ.** Extracellular oxidation in cystic fibrosis airway epithelium causes enhanced EGFR/ADAM17 activity. *Am J Physiol Lung Cell Mol Physiol* 314: L555–L568, 2018. doi:10.1152/ajplung.00458.2017.
47. **Wang S, Zhang Y, Wang Y, Ye P, Li J, Li H, Ding Q, Xia J.** Amphiregulin confers regulatory T cell suppressive function and tumor invasion via the EGFR/GSK-3β/Foxp3 axis. *J Biol Chem* 291: 21085–21095, 2016. doi:10.1074/jbc.M116.717892.
48. **Warren KJ, Wyatt TA, Romberger DJ, Ailts I, West WW, Nelson AJ, Nordgren TM, Staab E, Heires AJ, Poole JA.** Post-injury and resolution response to repetitive inhalation exposure to agricultural organic dust in mice. *Safety (Basel)* 3: 10, 2017. doi:10.3390/safety3010010.
49. **Waters DW, Blokland KEC, Pathinayake PS, Burgess JK, Mutsaers SE, Prele CM, Schuliga M, Grainge CL, Knight DA.** Fibroblast senescence in the pathology of idiopathic pulmonary fibrosis. *Am J Physiol Lung Cell Mol Physiol* 315: L162–L172, 2018. doi:10.1152/ajplung.00037.2018.
50. **Weiss DJ, Chambers D, Giangreco A, Keating A, Kotton D, Lelkes PI, Wagner DE, Prockop DJ; ATS Subcommittee on Stem Cells and Cell Therapies.** An official American Thoracic Society workshop report: stem cells and cell therapies in lung biology and diseases. *Ann Am Thorac Soc* 12: S79–S97, 2015. doi:10.1513/AnnalsATS.201502-086ST.
51. **Wells AD, Poole JA, Romberger DJ.** Influence of farming exposure on the development of asthma and asthma-like symptoms. *Int Immunopharmacol* 23: 356–363, 2014. doi:10.1016/j.intimp.2014.07.014.
52. **Wunschel J, Poole JA.** Occupational agriculture organic dust exposure and its relationship to asthma and airway inflammation in adults. *J Asthma* 53: 471–477, 2016. doi:10.3109/02770903.2015.1116089.
53. **Xia H, Diebold D, Nho R, Perlman D, Kleidon J, Kahm J, Avdulov S, Peterson M, Nerva J, Bitterman P, Henke C.** Pathological integrin signaling enhances proliferation of primary lung fibroblasts from patients with idiopathic pulmonary fibrosis. *J Exp Med* 205: 1659–1672, 2008. doi:10.1084/jem.20080001.
54. **Xu Q, Chiao P, Sun Y.** Amphiregulin in cancer: new insights for translational medicine. *Trends Cancer* 2: 111–113, 2016. doi:10.1016/j.trecan.2016.02.002.
55. **Xu Y, Meng C, Liu G, Yang D, Fu L, Zhang M, Zhang Z, Xia H, Yao S, Zhang S.** Classically activated macrophages protect against lipopolysaccharide-induced acute lung injury by expressing amphiregulin in mice. *Anesthesiology* 124: 1086–1099, 2016. doi:10.1097/ALN.0000000000001026.